

E. L. Papazoglou, N. E. Karkalos,
A. P. Markopoulos, Athens, Greece,
P. Karmiris-Obratański, Cracow, Poland

ON THE MACHINING OF ALUMINUM ALLOY AL6063 WITH EDM

Abstract. *Electrical Discharge Machining (EDM) is a non-conventional machining process, which allows the machining of any electrical conductive material, regardless its mechanical properties, with high dimensional accuracy, and in complex shapes and geometries. EDM widely utilized by modern industry, taking advantage of its unique inherent capabilities. Aluminum alloys find extensive use in numerous applications, and their machining consist an interesting topic, with tangible industrial interest. The current study presents an experimental investigation of machining Al6063 alloy with EDM. A full scale experiment was conducted, with control parameters the pulse-on current and time. The productivity of the process calculated based on the Material Removal Rate (MRR), while the Surface Roughness of the machined surfaces was estimated in terms of R_a and R_z . For these performance indexes Analysis Of Variance was performed and semi-empirical relations that correlate machining parameters with obtained results were proposed. Finally, the cross sections of the specimens were observed in optical microscopy, in order the formation of the White Layer to be studied.*

Keywords: *Electrical Discharge Machining; Aluminum alloys; Material Removal Rate; Surface Roughness; pulse-on current and time; White Layer; Analysis of Variance.*

INTRODUCTION

Electrical Discharge Machining (EDM) is classified as a non-conventional machining process, which utilizes repetitive rapid sparks to remove material from the workpiece. A pulsed voltage difference is applied between the working electrode and the workpiece, both of which been submerged into a dielectric medium. Under specific conditions of voltage difference and gap distance between electrode and workpiece, the insulating effect of the electric fluid breaks down, resulting a single spark to be discharged. This spark forms a plasma channel between the electrode and the workpiece, with reached temperatures in the range of 6000-12000K. Thermal energy from this plasma channel is absorbed by the electrode and the workpiece, causing material to melt and ablate. At the end of the pulse, the plasma channel collapses, and the electrode - workpiece system returns to its initial state. From every spark, a tiny crater is formed, with the removed material volume been in the range of 10^{-6} - 10^{-4} mm³; the total material removal is resulted by thousands, even millions of consecutive sparks [1], [2]. Although EDM is a multiparameter process the most significant control parameters are the pulse-on current (I_p) and the pulse-on time (T_{on}) [3]. EDM is widely used in modern industrial environment, since it is a non-contact material removal process,

capable to handle any electrical conductive material, regardless its mechanical properties.

Moreover, by utilizing EDM, high dimensional accuracy can be obtained, in complex shapes and geometries. EDM finds extensive applicability in aerospace, automotive, biomedical and die industry [4]. Finally, the process performance is mainly measured in terms of Material Removal Rate (MRR), Tool Wear Ratio (TWR), and machined Surface Roughness (SR), by often employing the R_a and R_t indexes [5].

Aluminum alloys are widely employed in numerous of industrial applications, hence, in addition to the conventional machining methods, EDM is utilized in their machining, especially where high quality standards are required. In the work of Khan [6] the MRR and the electrode wear were studied during machining aluminum and mild steel with EDM by using copper and brass working electrodes. It was verified the dependence of the machining performances from the electrode and workpiece material, and the pulse-on current. Gatto et al. [7] conducted research concerning the performance optimization in machining aluminum alloys for moulds production with EDM. Namely, the Al2219-T6, Al7050-T6, and Al7075-T6 alloys were studied, in roughing, semifinishing and finishing machining operations, while the machining performances were estimated in terms of dimensional accuracy and surface roughness. According to the relevant literature, the aluminum alloy 6 series gathers research interest. Arooj et al. [8] studied the effect of pulse-on current in machining Al6061-T6 with EDM, focusing mainly on the MRR and the obtained surface roughness and morphology. Al6061 was also studied by Pramarik et al. [9] in its machining with EDM, by employing graphite electrode and two different dielectric mediums, paraffin oil and distilled water. Again their research was mainly focused on the MRR, the electrode wear, and the surface quality. The surface quality was estimated in terms of surface roughness, and Average White Layer Thickness (AWLT). The machining of aluminum alloys with EDM becomes even more interest topic considering that aluminum alloys are utilized as metal matrix in composite materials, and EDM consist a feasible and efficient method in machining these kind of materials [10]–[12]. For example, Radhika et al. [13] presented a study regarding the optimization of EDM parameters in machining aluminum hybrid composites by using the Taguchi method. The experiment control parameters were the pulse-on current, the pulse-on time, and the dielectric fluid flushing pressure, while the machining performances were estimated in terms of MRR, TWR, and R_a .

The current paper presented an experimental investigation of machining aluminum alloy 6063 with EDM. Al6063 is one of the most commonly used aluminum alloys, with a wide range of applications. The experiments were carried out to investigate how the pulse-on current and time affect the MRR and the machined Surface Roughness. The SR was estimated in terms of R_a and R_t , while the surfaces' cross

sections were observed through optical microscopy in order the formation of White Layer to be studied. Finally, for the aforementioned machining performances indexes Analysis of Variance (ANOVA) was performed and semi-empirical relations that correlate machining parameters with results were proposed.

EXPERIMENTAL PROCEDURE

Experiments were carried out on an ANGIETRON EMT 1.10 die sinking EDM machine using plates of aluminum 6063 as workpiece material. Chemical composition and basic thermo-physical properties of Al6063 alloy are presented in table 1. In the experiments a copper electrode with nominal dimensions of 38x23mm was utilized, while the electrode was cleaned between the experiments in order to avoid any depositions accumulation on its surface. Highly purified synthetic hydrocarbon oil was applied as dielectric medium that was properly channeled into the working tank for efficient debris removal. Finally, in order a full surface morphology to be formed a nominal 1mm cut depth was set. A full-scale experiment was carried out for pulse-on current and time from 15 up to 24A and from 100 up to 500 μ s respectively. In table 2 the machining parameters are listed in details. The machining voltage was kept constant, specifically, 100 and 30V the open and close circuit voltage respectively. The Duty Factor (η) was automatically adjusted by the machine, and could be indirectly estimated based on the mean current. Taking in mind that voltage pulses can approximated by square pulses, the Duty Factor is calculated based on eq. 1:

$$\eta = \frac{\bar{I}_p}{I_p} \quad (1)$$

with \bar{I}_p with the ammeter indication of the mean current intensity in A and I_p the nominal pulse-on current in A.

The MRR is defined as the volume of the removed material per minute, and calculated based on eq. 2:

$$MRR = \frac{W_{st} - W_{fin}}{\rho \cdot t_m} \quad (2)$$

with MRR the material removal ratio in gr/min, W_{st} , W_{fin} the workpiece weight before and after machining, respectively, in gr, ρ the workpiece material density in gr/mm³ and t_m the machining time in min.

The average (R_a) and the maximum (R_t) surface roughness were calculated as the mean value of five consecutive measurements on each machined surface. Furthermore, the machined surfaces cross sections were grinded, polished and chemically treated with proper etchant, being composed of 92ml distilled water, 6ml nitric acid and 2ml hydrofluoric acid and the etched surfaces were observed in optical microscope. Finally for all the aforementioned measured and/or calculated

indexes, ANOVA was performed and semi-empirical correlations between machining parameters and results were proposed.

Table 1 – Al6063 chemical composition and thermo-physical properties

Component Wt%	Al (max)	Cr (max)	Cu (max)	Fe (max)	Mg	Mn (max)	Si	Ti (max)	Zn (max)
	97.5	0.1	0.1	0.35	0.45-0.9	0.1	0.2-0.6	0.1	0.1
Physical Properties	Density (g/mm ³)		Electrical Resistivity (ohm/m)		Specific Heat Capacity (kJ/kgK)		Thermal Conductivity (W/mk)		Melting Point (K)
	0,0027		3.32e-4		0.9		200		908

Table 2 – Machining parameters

Machining Conditions	Level 1	Level 2	Level 3	Level 4
Discharge current I _p (A)	15	18	21	24
Pulse on-Time T _{on} (μs)	100	200	300	500
Dielectric	Synthetic Hydrocarbon Fluid			
Dielectric Flushing	Side Flushing			
Open circuit Voltage (V)	100			
Close circuit Voltage (V)	30			

RESULTS AND DISCUSSION

Table 3 – Experimental results

I _p (A)	T _{on} (μs)	MRR (mm ³ /min)	Ra (μm)	Rt (μm)
15	100	125,66	8,10	53,40
18	100	189,49	9,30	62,40
21	100	148,15	9,10	64,80
24	100	211,64	10,30	77,60
15	200	139,65	11,20	67,80
18	200	189,30	12,40	88,60
21	200	194,00	11,80	83,40
24	200	233,92	13,40	85,80
15	300	129,63	14,20	89,20
18	300	161,62	14,20	96,40
21	300	189,30	13,80	101,00
24	300	219,91	15,00	94,00
15	500	133,10	13,70	94,80
18	500	177,13	16,00	101,40
21	500	170,37	13,60	85,80
24	500	202,82	16,70	110,20

In table 3 – the experimental results are presented, based on which the following ANOVA was performed.

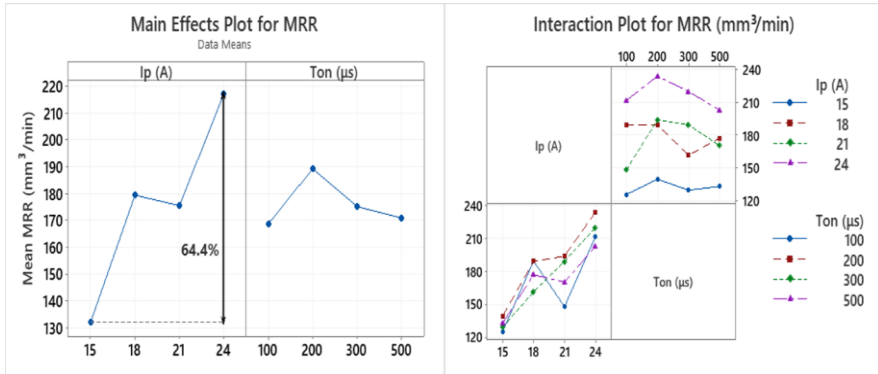


Figure 1 – Main Effects Plot and Interaction Plot for MRR

In figure 1 the Main Effects Plot and the Interaction Plot of MRR are presented. As it is clearly deduced, the pulse-on current has the main and major effect on MRR, while pulse-on time slightly and vaguely affects the MRR. More specifically, as the I_p increased from 15 to 18A the MRR for all pulse-on times increased, while a further increase up to 21A resulted a stabilization, even a slight reduction, in MRR. The increase in pulse-on current to 24A was followed by an increase in MRR, with the mean MRR for 24A be 64.4% higher than for 15A. On the other hand, the pulse-on time seems to have a fuzzy and insignificant influence on MRR. Based on a non-linear regression model, the MRR is correlated with pulse-on current and time according to eq. 3:

$$MRR = 11.373 I_p^{0.9229} T_{on}^{-0.0002} \quad (3)$$

with MRR in mm^3/min , I_p in A and T_{on} in μs .

The correlation level is considered adequate, with S-value 18.31; moreover, in figure 2 the MRR experimental results and those predicted from the regression model are juxtaposed, confirming the sufficient correlation. Finally, the major effect of I_p on MRR is also confirmed by the eq. 3, where the exponents of pulse-on current and time differ orders of magnitude indicating the significance of I_p .

On the contrary of MRR, for SR the major parameter is the pulse-on time. In figure 3 the Main Effects Plot and the Interaction Plot of R_a are presented. It is clear that increase in T_{on} results an increase in R_a , while the pulse-on current does not affect the R_a in a consistent way. Namely, as the T_{on} increased from 100 to 500 μs the mean R_a increased 63%, from around 9 μm to 15 μm .

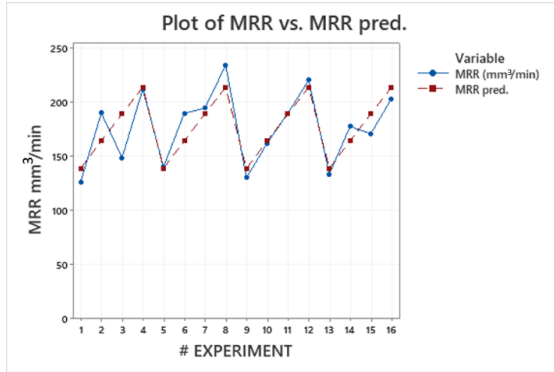


Figure 2 – MRR experimental results vs. predicted ones

On the other hand, increase in I_p resulted both increase and decrease of R_a , depending on the combination of pulse-on current and time. By a more detailed analysis, and based on the Interaction Plot diagram, the constant increase of MRR for higher pulse-on times is confirmed, with only an exception for 15A and 21A and for pulse-on time 500 μ s, where a slight different behavior is observed. Nevertheless, this does not affect the general rule, namely, that the R_a is mainly affected by the T_{on} , increase of which results an increase in R_a .

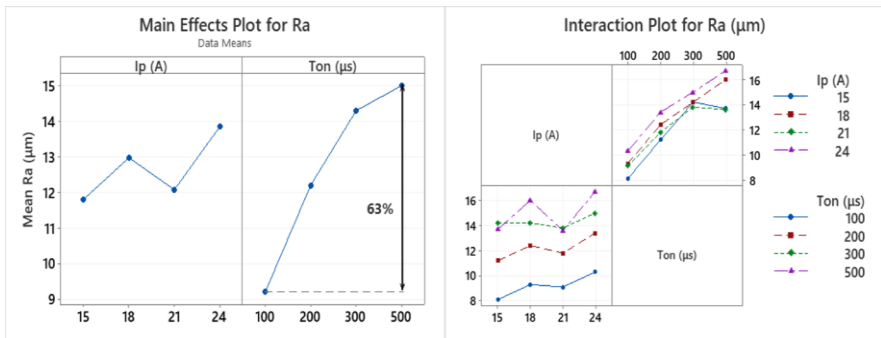


Figure 3 – Main Effects Plot and Interaction Plot for Ra

Again, it is of extreme interest the capability to predict the R_a based on the machining parameters, i.e. the pulse-on current and time. Thus, a semi-empirical relation is proposed, based on the Response Surface Method (RSM). Considering the linear, quadric, and interaction terms, eq. 4 was emerged:

$$Ra = 7.68 - 0.471I_p + 0.0473T_{on} + 0.0167I_p^2 - 0.000054T_{on}^2 - 0.000013I_pT_{on} \quad (4)$$

with R_a in μm , I_p in A and T_{on} in μs . The correlation is adequate, with R-sq 92.05% and S value 0.87. Moreover, the good fit of the model is confirmed by the juxtaposition of experimental and by the model predicted values of R_a in figure 4.

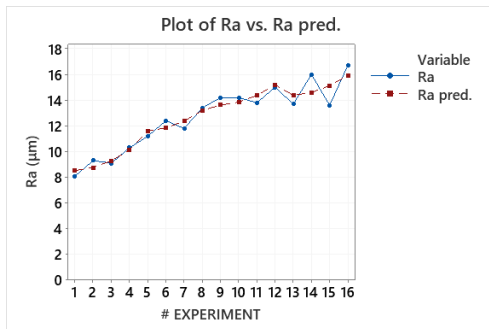


Figure 4 – R_a experimental results vs. predicted ones

Similarly to R_a , the R_t follows the same general rule, namely, it is mostly affected by the pulse-on time, while the pulse-on current seems to have a vague affect on it. In figure 5 the Main Effects Plot along with the Interaction Plot for R_t are presented. An important observation is that plots of R_a and R_t follow almost the same pattern, implying and confirming the existed strong correlation between them. As the pulse-on time increases from 100 to 500 μs , the mean R_t increases too, by almost 52%. The Interaction Plot corroborates this trend, with only one exception, and specifically, for 21A and 500 μs the R_t was slightly decreased. On the other hand, the increase in I_p results both increase and decrease of R_t , depending on the combination of the machining parameters, thus, any safe and reliable conclusion concerning the affect of pulse-on current on R_t can not be deduced.

The capability to predict the resulted R_t depending on the machining conditions is extremely important and helpful, since R_t is straight related with quality and functionality issues. To correlate the R_t with the pulse-on current and time, for once more, the RSM method was employed. By adopting a model that includes linear, quadric and interaction terms, the semi-empirical correlation of eq. 5 was emerged:

$$Rt = -36.4 + 5.41I_p + 0.3525T_{on} - 0.076I_p^2 - 0.000329T_{on}^2 - 0.00359I_pT_{on} \quad (5)$$

with R_t in μm , I_p in A and T_{on} in μs . The fit of the proposed model is considered adequate, with R-sq 86.05% and S Value 7.25. The good correlation it is further

confirmed by the juxtaposition in figure 5 of the experimentally measured and the predicted values of R_t .

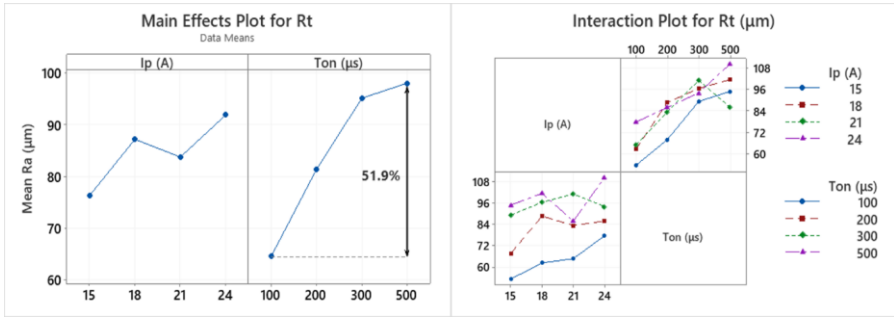


Figure 5 – Main Effects Plot and Interaction Plot for R_t

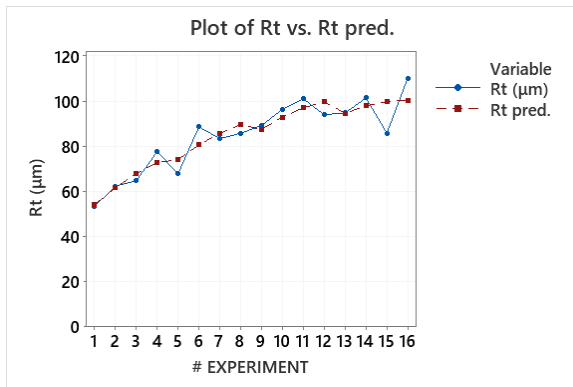


Figure 6 – R_t experimental results vs. predicted ones

During machining with EDM, and as it has already been mentioned, the occurring sparks melt and/or ablate material from the workpiece, forming tiny craters. Nevertheless, only a proportion of the molten material is finally removed by the workpiece, with the rest of it remaining on the workpiece, being re-solidified forming a layer of amorphous material. Additionally, removed and/or ablated material that remained in a close approximation on the surface, it may re-condensed and being deposited on it. This way, a layer of material is formed, well known as White Layer, having different properties from the mother material. WL is differentiated in its thickness and characteristics depending on the machining

parameters, and namely the pulse-on current and time. The machining power, and the per pulse energy significantly affect the WL thickness, with the more intense machining conditions to lead in a thicker WL. Because of the high gradients in temperature and pressure that being developed on the surface, the WL is not always uniform and continuous. In figures 7 and 8 the cross sections of the workpiece for different machining conditions are presented.

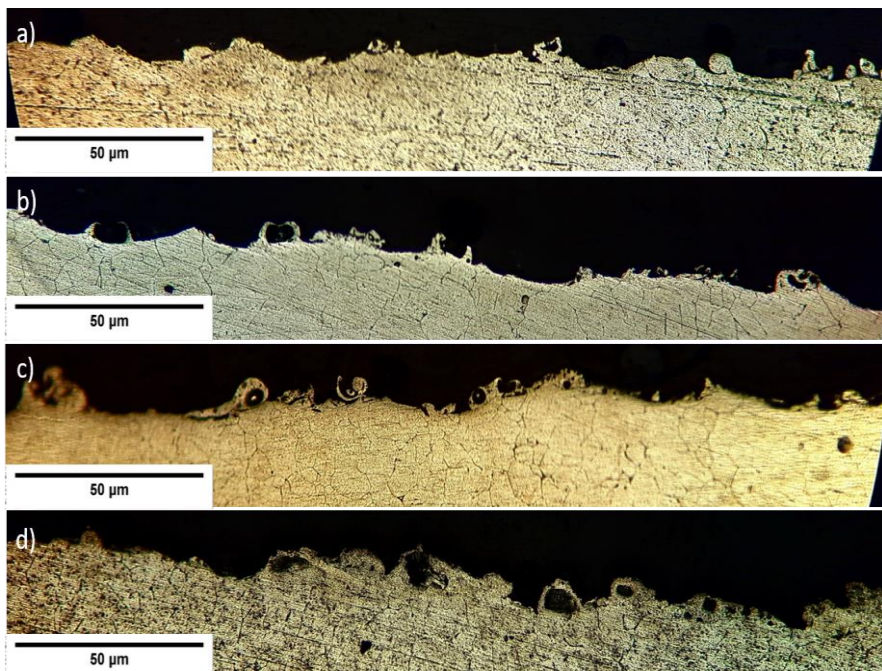


Figure 7 – Machined surface cross sections for 24A and pulse-on time
a) 100 μ s, b) 200 μ s, c) 300 μ s, a) 500 μ s

The dependence of the WL thickness and its characteristics on the machining conditions is confirmed by the cross section microscopy images that been presented in figure 7. With pulse-on current to remain constant, as the pulse-on time increases the WL becomes thicker, while, some new characteristics are appeared. For T_{on} 100 μ s the WL is very thin, with some randomly placed formations along its length. For pulse-on time 200 μ s the WL remains thin, but some hollow formations are emerged. For T_{on} 300 μ s, a thicker and more uniform WL is formed, while these hollow formations become denser and more bulky.

Finally, for pulse-on time $500\mu\text{s}$, a thick continuous WL has been formed, including hollow and bulky formations. These globules of material being shaped because during the rapid material's re-solidification, gases are trapped inside it, resulting these hollow formations. The more intense the machining parameters are, the more bulky and denser these globules become.

In figure 7, the formation of the WL was depicted, as the machining power was kept constant and the per pulse energy being increased (i.e. the pulse-on current was constant and equal to 24A, while the pulse-on time varied from 100 up to $500\mu\text{s}$). In figure 8, both, the machining power and the per pulse energy are changing. Similar observations can be made; namely, the WL for the more intense machining conditions become thicker, incorporating more bulky hollow globules. For the low pulse-on currents of 15 and 18A, the WL does not have any uniformity, but is appeared more like randomly spread formations. A degree of uniformity is emerged for higher machining powers, where the hollow globules seems to cover major part of the cross section.

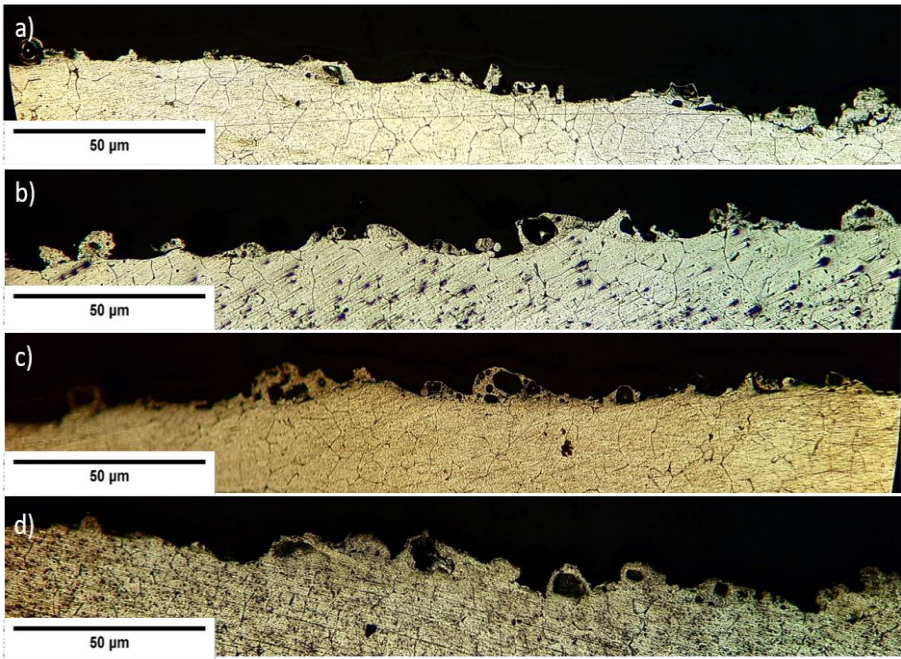


Figure 8 – Machined surface cross sections for $500\mu\text{s}$ and pulse-on current
a) 15A, b) 18A, c) 21A, a) 24A

CONCLUSIONS

In the current paper an experimental investigation of machining aluminum alloy Al6063 with EDM was presented. A full scale experiment was conducted, with control parameters the pulse-on current and time. The productivity of the machining was calculated based on the MRR, while the surface roughness was estimated in terms of R_a and R_t . For these performance indexes, ANOVA was performed, and semi-empirical relations that correlate machining parameters with its results were proposed. Finally the WL formation was studied through optical microscopy, where the specimens cross sections were observed. The main conclusions of the current study are:

- The MRR is mainly affected by the pulse-on current, as an increase in I_p results an increase in MRR. The pulse-on time has a vague and minor affect on MRR.
- The SR mostly depends on the pulse-on time. Specifically, increase in T_{on} leads in increase in R_a and R_t . On the other hand, the pulse-on time has a fuzzy influence on SR, hence, no reliable conclusions can be deduced.
- The formation of WL is affected on the machining power, and the per pulse energy. For higher machining power, and pulse energy the WL becomes thicker, while in the more intense machining parameters hollow globules being formed.

References. 1. *M.P. Jahan, Electrical Discharge Machining (EDM): Types, Technologies and Applications.* New York: Nova Science Publishers, 2015. 2. *E.C. Jameson, Electrical discharge machining.* Michigan: Society of Manufacturing Engineers, 2001. 3. *J. E. A. Qudeiri, A. I. Mourad, A. Ziout, M. H. Abidi, and A. Elkaseer,* "Electric discharge machining of titanium and its alloys: review," 2018. 4. *N. M. Abbas, D. G. Solomon, and F. Bahari,* "A review on current research trends in electrical discharge machining," vol. 47, pp. 1214–1228, 2007, doi: 10.1016/j.ijmachtools.2006.08.026. 5. *S. Choudhary and R. Jadoun,* "Current advanced research development of electric discharge machining (EDM): a review," *Int. J. Res. Advent Technol.*, vol. 2, no. 3, pp. 273–297, 2014. 6. *A. A. Khan,* "Electrode wear and material removal rate during EDM of aluminum and mild steel using copper and brass electrodes," *Int. J. Adv. Manuf. Technol.*, vol. 39, no. 5–6, pp. 482–487, 2008, doi: 10.1007/s00170-007-1241-3. 7. *A. Gatto, E. Bassoli, and L. Iuliano,* "Performance Optimization in Machining of Aluminium Alloys for Moulds Production: HSM and EDM," in *Aluminium Alloys Theory and Applications*, T. Kvackaj, Ed. IntechOpen, 2011. 8. *S. Arooj, M. Shah, S. Sadiq, S. H. I. Jaffery, and S. Khushmood,* "Effect of Current in the EDM Machining of Aluminum 6061 T6 and its Effect on the Surface Morphology," *Arab. J. Sci. Eng.*, vol. 39, no. 5, pp. 4187–4199, 2014, doi: 10.1007/s13369-014-1020-z. 9. *A. Pramanik, A. K. Basak, M. N. Islam, and G. Littlefair,* "Electrical discharge machining of 6061 aluminium alloy," *Trans. Nonferrous Met. Soc. China (English Ed.)*, vol. 25, no. 9, pp. 2866–2874, 2015, doi: 10.1016/S1003-6326(15)63912-7. 10. *P. Srikanth and C. P. Kumar,* "Electrical discharge machining characteristics of metal matrix composites-A Review," *Int. J. Sci. Res.*, vol. 4, no. 6, pp. 1385–1394, 2015, [Online]. Available: <http://www.sciencedirect.com/science/article/pii/S0924013600008232>. 11. *B. C. Kandpal, J. kumar, and H. Singh,* "Machining of Aluminium Metal Matrix Composites with Electrical Discharge Machining - A Review," *Mater. Today Proc.*, vol. 2, no. 4–5, pp. 1665–1671, 2015, doi: 10.1016/j.matpr.2015.07.094. 12. *L. Selvarajan, J. Rajavel, V. Prabakaran, B. Sivakumar, and G. Jeeva,* "A Review Paper on EDM

Parameter of Composite material and Industrial Demand Material Machining,” Mater. Today Proc., vol. 5, no. 2, pp. 5506–5513, 2018, doi: 10.1016/j.matpr.2017.12.140. 13. N. Radhika, A. R. Sudhamshu, and G. K. Chandran, “Optimization of Electrical Discharge Machining Parameters of Aluminium Hybrid Composites Using Taguchi Method,” J. Eng. Sci. Technol., vol. 9, no. 4, pp. 502–512, 2014.

Емануїл П. Папазоглу, Ніколаос Е. Каркалос,
Ангелос П. Маркопулос, Афіни, Греція,
Панагіотіс Карміріс-Обратанські, Краків, Польща

ПРО ОБРОБКУ АЛЮМІНІЄВОГО СПЛАВУ 6063 ЕЛЕКТРОЕРОЗІЙНИМ СПОСОБОМ.

Анотація. *Електроерозійна обробка (EDM) – це нетрадиційний процес механічної обробки, який дозволяє обробляти будь-який електропровідний матеріал, незалежно від його механічних властивостей, з високою точністю розмірів і складністю форми і геометрії. EDM широко використовується в сучасній промисловості, враховуючи його унікальні можливості. Алюмінієві сплави знаходять широке застосування в багатьох сферах, і їх обробка являє собою цікаву тему, що має відчутний промисловий результат. Ця робота представляє собою експериментальне дослідження обробки металу Al6063 електроерозійним способом. Було проведено повномасштабний експеримент з контрольними параметрами: енергією імпульсів і часом дії імпульсів. Продуктивність процесу розраховувалася на основі швидкості видалення матеріалу (MRR), в той час як шорсткість оброблених поверхонь оцінювалася в одиницях R_a і R_t . Для показників продуктивності був проведений дисперсійний аналіз і запропоновані напівемпіричні залежності, які корелюють параметри обробки з отриманими результатами. Нарешті, поперечні перерізи зразків вивчали за допомогою оптичної мікроскопії, щоб визначити виникнення «білого шару». Основні висновки цього дослідження такі: На MRR в основному впливає імпульсний струм, так як збільшення сили струму імпульсу I_p призводить до збільшення MRR. Час дії імпульсу T_{on} має невизначений і незначний вплив на MRR. Шорсткість поверхні в основному залежить від часу T_{on} . Зокрема, збільшення T_{on} призводить до збільшення R_a і R_t . З іншого боку, час T_{on} нечітко впливає на SR, тому не можна зробити ніяких надійних висновків. На формування «білого шару» (WL) впливає потужність обробки і енергія в імпульсі. Для більшої потужності обробки та енергії імпульсу WL стає товще, в той час як при більш інтенсивних параметрах обробки утворюються порожні глобули.*

Ключові слова: *електро-ерозійна обробка; сплави алюмінію; швидкість видалення матеріалу; шорсткість поверхні; енергія імпульсу і час дії; «білий шар»; аналіз дисперсії.*